

Mathematical analysis demonstrates that interferons- β and - γ interact in a multiplicative manner to disrupt herpes simplex virus replication

William P. Halford^{a,*}, Keith J. Halford^b, Amy T. Pierce^a

^aDepartment of Microbiology and Immunology, Tulane University Health Sciences Center, New Orleans, LA 70112, USA

^bDepartment of Water Resources, United States Geological Survey, Carson City, NV 89706, USA

Received 19 August 2004; received in revised form 10 November 2004; accepted 6 December 2004

Communicated by Robert Root-Bernstein

Available online 25 January 2005

Abstract

Several studies suggest that the innate interferons (IFNs), IFN- α and IFN- β , can act in concert with IFN- γ to synergistically inhibit the replication of cytomegalovirus and herpes simplex virus type 1 (HSV-1). The significance of this observation is not yet agreed upon in large part because the nature and magnitude of the interaction between IFN- α/β and IFN- γ is not well defined. In the current study, we resolve this issue by demonstrating three points. First, the hyperbolic tangent function, $\tanh(x)$, can be used to describe the individual effects of IFN- β or IFN- γ on HSV-1 replication over a 320,000-fold range of IFN concentration. Second, pharmacological methods prove that IFN- β and IFN- γ interact in a greater-than-additive manner to inhibit HSV-1 replication. Finally, the potency with which combinations of IFN- β and IFN- γ inhibit HSV-1 replication is accurately predicted by multiplying the individual inhibitory effects of each cytokine. Thus, IFN- β and IFN- γ interact in a multiplicative manner. We infer that a primary antiviral function of IFN- γ lies in its capacity to multiply the potency with which IFN- α/β restricts HSV-1 replication in vivo. This hypothesis has important ramifications for understanding how T lymphocyte-secreted cytokines such as IFN- γ can force herpesviruses into a latent state without destroying the neurons or leukocytes that continue to harbor these viral infections for the lifetime of the host.

© 2005 Elsevier Ltd. All rights reserved.

Keywords: Interferon; Synergy; Multiplicative interaction; Herpesvirus; Latent infection

1. Introduction

Interferon (IFN)- α , IFN- β , and IFN- γ are secreted proteins that play important roles in host resistance to viral infections. IFN- α and/or IFN- β (IFN- α/β) are secreted by most cells as an innate response to viral infection, and both bind to the IFN- α/β receptors that are expressed on all nucleated cells (Vilcek and Sen, 1996). IFN- γ shares no amino acid homology with IFN-

α/β , binds to a distinct receptor, and its in vivo production is tightly regulated and restricted to professional antigen-presenting cells, natural killer cells, or T cells (Farrar and Schreiber, 1993; Lieberman and Hunter, 2002; Suzue et al., 2003). Activation of IFN- α/β receptors or IFN- γ receptors, which are present on all cells in the body, transduces a signal to the nucleus via Janus kinases and the phosphorylation of Stat1 and Stat2. These events lead to the formation of transcriptional complexes such as ISGF-3 and IRF-1, which induce IFN-stimulated gene expression in the cell (Levy and Darnell, 2002; Matsumoto et al., 1999; Varinou et al., 2003). The literature often suggests that the IFN- α/β and IFN- γ signaling pathways are more redundant than they are different. However, if this is true, why is IFN- γ -

*Corresponding author. Department of Veterinary Molecular Biology, Montana State University, 960 Technology Boulevard, Bozeman, MT 59718, USA. Tel.: +1 406 994 6374; fax: +1 406 994 4303.

E-mail address: halford@montana.edu (W.P. Halford).

induced activation of Stat1 dependent on the IFN- α/β receptor, and why are IFN- α/β receptors and IFN- γ receptors physically associated in the cell (Takaoka et al., 2000)?

Numerous observations made in the 1980s and 1990s suggested that the innate IFNs (α/β) can act in concert with IFN- γ to synergistically inhibit HSV-1 replication in vitro (Balish et al., 1992; Chen et al., 1993; Czarniecki et al., 1984; Neumann-Haefelin et al., 1985; Zerial et al., 1982). If correct, such observations would indicate that the IFN- α/β and IFN- γ pathways are not purely redundant, but rather reinforce one another. These observations remained obscure for many years because the biological significance of the interaction between IFN- γ and the innate IFN system was never validated in vivo. Recently, our research led us to re-discover that combinations of IFN- α/β and IFN- γ inhibit HSV-1 replication in vitro with a potency that greatly exceeds that which would be expected if IFN- α/β and IFN- γ were purely redundant (Sainz and Halford, 2002). On the heels of this observation, two recent in vivo studies suggest that the interaction between the IFN- α/β and IFN- γ pathways is functionally relevant in host control of HSV-1 infection (Luker et al., 2003; Vollstedt et al., 2004).

Co-activation of IFN- α/β receptors and IFN- γ receptors may be sufficient to effectively stop the spread of herpesviruses in vivo. Like many cooperative interactions between the innate and adaptive immune response (Chehimi and Trinchieri, 1994; MacLennan and Vinuesa, 2002), such a hypothesis would suggest that the second signal provided by IFN- γ might serve to multiply the potency with which IFN- α/β (i.e. the first signal) restricts herpesvirus replication in host cells. Such a hypothesis might explain the rapidity with which viral antigen expression ceases when IFN- γ secreting T cells infiltrate HSV-infected tissues (Halford et al., 1996; Koelle et al., 1998; Liu et al., 1996; Simmons and Tschärke, 1992; Speck and Simmons, 1998). There is considerable appeal in the simplicity of the hypothesis and its consistency with the in vivo data. However, the interaction by which IFN- α/β and IFN- γ inhibit HSV-1 replication remains poorly defined. The claim that the interaction between IFN- α/β and IFN- γ is synergistic (i.e. greater than dose-additive) has not been substantiated using established pharmacological methods. Moreover, a recent comparison of the effects of IFN- α and/or IFN- γ led the investigators to conclude that the ‘low-level activity of exogenous IFNs [on HSV-1 replication] may be additive’ (Chee et al., 2003). Therefore, the available evidence neither proves, nor disproves, the hypothesis that IFN- γ acts to multiply the antiviral efficacy with which IFN- α/β inhibits HSV-1 replication in vivo.

We initiated the current study to resolve this issue. Many methods are described in the literature for

determining whether an interaction between two biologically active agents is additive or synergistic (Berenbaum, 1989; Dressler et al., 1999; Gebhart, 1992; Greco et al., 1995; Prichard and Shipman, 1990; Slinker, 1998; Suhnel, 1990, 1992; Tallarida, 2000, 2001; Tallarida et al., 1997). However, we were unable to extract a simple and logical method from the literature by which the interaction between IFN- β and IFN- γ could be defined. What follows represents our own solution to the problem, which we achieved by addressing the three following goals:

1. Develop a mathematical model that describes the individual effects of IFN- β or IFN- γ on HSV-1 replication over an essentially infinite range of ligand concentration.
2. Determine if a null hypothesis of dose-additivity can account for the potency with which combinations of IFN- β and IFN- γ inhibit HSV-1 replication. If not,
3. Develop a model that mathematically combines the individual effects of IFN- β and IFN- γ in a manner that accurately describes their combined effects on HSV-1 replication.

The results of this analysis demonstrate that combinations of IFN- β and IFN- γ interact in a multiplicative manner to inhibit HSV-1 replication. We infer that the T cell-secreted cytokine IFN- γ suppresses primary and recurrent HSV-1 infections in vivo (Cantin et al., 1999a,b; Khanna et al., 2003; Liu et al., 2001, 2000) by virtue of its capacity to multiply the efficacy with which the innate IFNs, IFN- α and/or IFN- β , inhibit viral replication

2. Materials and methods

2.1. Cells, viruses, and interferons

Vero cells (American Type Culture Collection, Manassas, VA) were propagated in Dulbecco's modified Eagle medium containing 0.15% HCO_3^- supplemented with 10% fetal bovine serum (FBS), penicillin G (100 U/ml), and streptomycin (100 mg/ml), hereafter referred to as “complete DMEM,” in a 37°C incubator that contained 5% CO_2 . Wild-type HSV-1 strain KOS (Smith, 1964) was propagated in Vero cells. Recombinant human (hu)-IFN- β and hu-IFN- γ were obtained from PBL Biomedical Laboratories (New Brunswick, NJ). IFNs were added to cultures 18 h prior to infection and IFN treatment was maintained continuously thereafter.

2.2. Dose–response analysis of the combined effects of interferons on HSV-1 replication

2.2.1. Additive composite curve analysis

Separate solutions of IFN- β or IFN- γ were serially diluted in 0.5 log increments in complete DMEM from a starting concentration of 10,000 U/ml down to a final concentration of 0.032 U/ml. Equipotent (1:1) combinations of IFN- β and IFN- γ were made by mixing one volume of each IFN- β dilution (e.g. 10,000 U/ml) with an equal volume of the corresponding IFN- γ dilution (e.g. 10,000 U/ml) to obtain mixtures that contained an equal total concentration of IFN (5000 U/ml each). Vero cells were seeded in 24-well plates at a density of 10^5 cells per well. Twenty-four hours later, the medium in each well was replaced with 0.5 ml complete DMEM containing dilutions of **1.** IFN- β , **2.** IFN- γ , or **3.** equipotent combinations of IFN- β and IFN- γ that ranged in concentration from 0 to 10,000 U/ml. After 18 h of IFN pre-treatment, a 20 μ l inoculum containing 30,000 PFU of HSV-1 strain KOS was added to the 0.5 ml culture medium present in each well to achieve an approximate MOI of 0.1 PFU per cell. At 30 or 48 h after inoculation, HSV-1 infected and uninfected cells were harvested for DNA dotblots.

2.2.2. Three-dimensional response surface analysis

Vero cells were treated with 0.33 log dilutions of IFN- β and 0.33 log dilutions of IFN- γ to yield an 8×8 matrix of 64 unique dosage combinations of IFN- β and IFN- γ , as follows. Separate solutions of IFN- β or IFN- γ were serially diluted in 0.33 log increments in complete DMEM from a starting concentration of 2000 U/ml down to a final concentration of 20 U/ml. Vero cells were seeded in 24-well plates at a density of 1×10^5 cells per well. Twenty-four hours later, the medium in eight groups of eight wells was replaced with 0.25 ml complete DMEM containing either 0, 20, 43, 94, 200, 430, 940, or 2000 U/ml of IFN- β . To each group of eight wells that received a single dose of IFN- β (e.g. 2000 U/ml), 0.25 ml of complete DMEM was added that contained 0, 20, 43, 94, 200, 430, 940, or 2000 U/ml of IFN- γ . Once the IFN- β and IFN- γ dilutions were combined, the final concentration of IFN- β or IFN- γ in each well was either 0, 10, 21, 47, 100, 215, 465, or 1000 U/ml. After 18 h of IFN pre-treatment, a 20 μ l inoculum containing 30,000 PFU of HSV-1 strain KOS was added to the 0.5 ml culture medium present in each well to achieve an approximate MOI of 0.1 PFU per cell. At 30 or 48 h after inoculation, HSV-1 infected and uninfected cells were harvested for DNA dotblots.

2.3. Dotblot analysis of viral DNA yields in HSV-1 infected Vero cells

At 30 or 48 h after inoculation, crude lysates were harvested from each well by removing culture medium

and dissolving the cells in 0.5 ml of 0.4 M NaOH/10 mM EDTA. These crude, DNA-containing lysates were thoroughly scraped from each well, transferred to a 0.6 ml microfuge tube, heated to 90 °C for 10 min, snap-cooled on ice, and blotted on Zeta Probe GT nylon membrane (BioRad Laboratories, Hercules, CA) in an 8×12 dotblot pattern using a Convertible™ vacuum filtration manifold (Whatman-Biometra, Grönningen, Germany). DNA samples were crosslinked to nylon membranes by irradiating with 0.2 J/cm² in a UV crosslinker (Spectronics Corporation, Westbury, NY) and were hybridized to a ³²P radiolabeled oligonucleotide specific for HSV-1 glycoprotein D (5'-aggccccagagactgtgttaggagcattcgggtgtactc-3'), which was end-labeled with [α -³²P] dATP using terminal deoxynucleotidyl transferase (Promega Corporation, Madison, WI). The probe was allowed 16 h to hybridize to the membrane at 42 °C in a solution containing 2 ng/ml labeled probe, 7% SDS, 120 mM Na₂HPO₄, and 250 mM NaCl. Excess probe was removed from membranes by sequential rinses in 0.1 \times standard saline citrate (SSC) containing 0.1% SDS and membranes were exposed to phosphor screens, which were scanned on a Cyclone Phosphor-Imager (Perkin Elmer Life Sciences, Boston, MA). The amount of radiolabeled probe hybridized to each DNA sample was determined using OptiQuant v4.0 software (Perkin Elmer Life Sciences). Each nylon membrane contained **1.** DNA samples from HSV-1 infected, IFN-treated test cultures, **2.** uninfected controls that defined background levels of hybridization and **3.** a 1/3rd-log (2.15-fold) dilution series of viral DNA that defined the relationship between the relative amount of HSV-1 DNA (x) and the amount of ³²P radiolabel (y) that hybridized to each sample. The standard curve was used to calculate the amount of viral DNA in each sample relative to the lower limit of detection of the assay, which was assigned a value of 1. Background was defined as the amount of signal associated with lysates of uninfected Vero cell samples. The standard curves used to derive log (HSV-1 DNA, x) from log (measured density units, y) was of the general form

$$x = x_{50} + \Delta x \operatorname{arctanh} \left(\frac{y - y_{50}}{\Delta y} \right).$$

For convenience, Microsoft Excel's trendline-fitting feature can also be used to rapidly define a third-order polynomial equation ($x = ay^3 + by^2 + cy + d$) that closely approximates the shape of the $x = \operatorname{arctanh}(y)$ function.

2.4. Quantitative and statistical analysis of dose–response data

Analysis of numerical data and statistical analyses were performed with the software package Microsoft Excel. Data are presented as the mean \pm standard

deviation (SD). The coefficient of variation within a group of replicates was calculated to be $100 \times$ standard deviation/mean. Parameters that define the IFN dose–response relation were estimated by minimizing the sum-of-squares differences between observed and predicted log (viral DNA yield). These differences were minimized using the “Solver” function in Microsoft Excel. The accuracy with which mathematical models predicted log (viral DNA yield) in Vero cells treated with IFN- β , IFN- γ , or combinations of IFN- β and IFN- γ was evaluated using a two-tailed paired *t*-test to determine the probability that the average residual difference between the predicted (*P*) and observed (*O*) values was equal to zero (i.e. $H_0 : P - O = 0$).

3. Results

3.1. Viral DNA yields provide a precise and accurate measure of HSV-1 replication

The following experiment was performed to determine if measurement of viral DNA yield in crude cell lysates provided a valid measure of HSV-1 replication efficiency. Vero cells were infected with 1/3rd log dilutions of HSV-1 that ranged in multiplicity of infection (MOI) from 0.002 to 4.6 PFU/cell. At 24 h post-inoculation (p.i.), viral titers were determined in one set of cultures (Fig. 1A). The other set of cultures was dissolved in a NaOH solution and viral DNA yields were measured based on the efficiency with which a virus-specific probe hybridized to dotblots of crude cell lysates (Fig. 1B and C). Viral titers were linearly proportional to the size of the viral inoculum between MOIs of 0.002 and 0.1 (Fig. 1A; $r^2 = 0.97$). Viral inoculum was not limiting at higher MOIs, and thus a plateau titer of $10^{7.3}$ PFU/ml was observed in all cultures infected with 0.2–4.6 PFU per cell (Fig. 1A). Likewise, viral DNA yields were linearly proportional to the size of the viral inoculum between MOIs of 0.002 and 0.1 ($r^2 = 1.00$), and reached a plateau in cultures infected with higher MOIs (Fig. 1B and C). Regression analysis indicated that at all MOIs tested, HSV-1 DNA yield was directly proportional to viral titers ($r^2 = 0.98$). Regarding the relative precision of the methods, the coefficient of variation of viral titers was $3.4 \pm 0.6\%$ and of viral DNA yields was $1.5 \pm 0.5\%$. Therefore, dotblot analysis of viral DNA yield provided a valid measure of HSV-1 replication efficiency.

3.2. Human IFN- β inhibits HSV-1 replication in a dose-dependent manner

Viral replication was compared in Vero cells inoculated with 0.1 PFU per cell of HSV-1 and which were treated with 0.032 to 10,000 U/ml of human IFN- β .

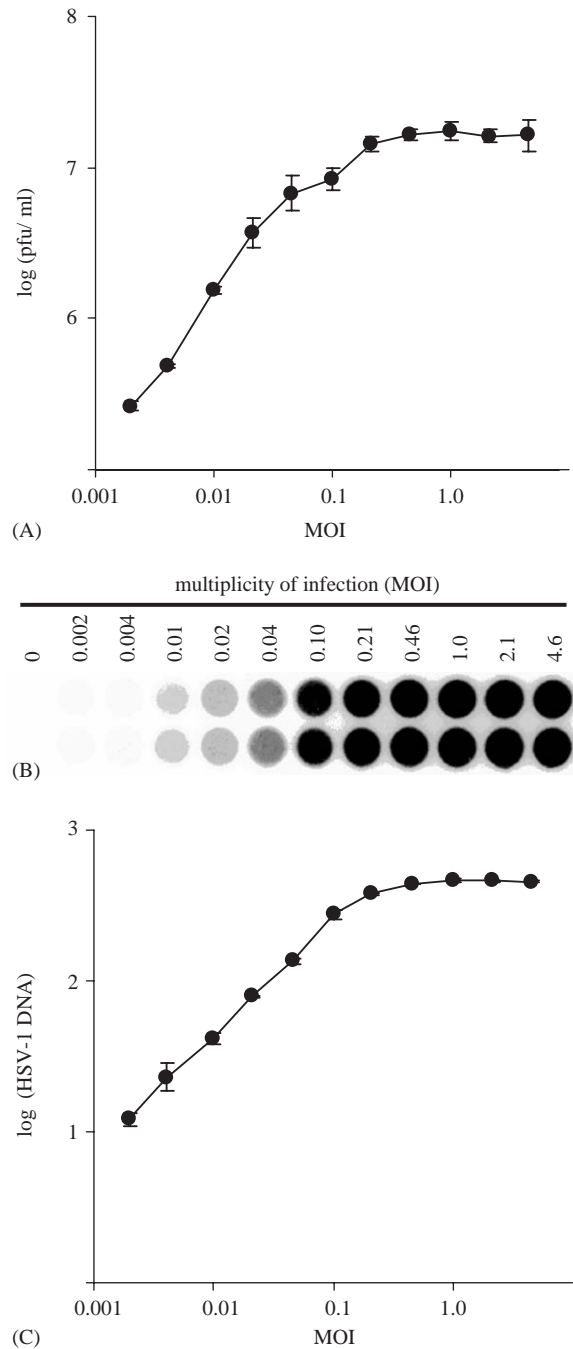


Fig. 1. Measurements of HSV-1 DNA yield correlate with viral titers. (A) HSV-1 titers were determined by plaque assay in Vero cells 24 h after inoculation with 0.002 to 4.6 PFU per cell ($n = 2$ per MOI). (B) Dotblots of DNA samples harvested from uninfected Vero cells (MOI = 0) and HSV-1 infected Vero cells 24 h after inoculation ($n = 2$ per MOI). Estimates of HSV-1 DNA yield were calculated based on the amount of HSV-specific oligonucleotide that hybridized to each DNA sample. (C) The log (viral DNA yield) is plotted as a function of MOI, and is expressed in terms of log (fold-increase above the lower limit of detection); thus, the value ‘0’ on the y-axis indicates the lower limit of detection of the assay.

When infected cells were harvested 30 h p.i., IFN- β concentrations of less than 10 U/ml had no effect on HSV-1 replication (Fig. 2A and C). Between doses of 10

and 1000 U/ml, viral DNA yields decreased in proportion to the IFN- β concentration in cell culture medium. At concentrations of ≥ 1000 U/ml, IFN- β reduced HSV-1 DNA yields by ~ 40 -fold (Fig. 2A and C). When the time of viral DNA harvest was delayed until 48 h p.i., IFN- β concentrations below 320 U/ml had no effect on HSV-1 DNA yields, and only an ~ 8 -fold reduction in HSV-1 DNA yield was achieved by 10,000 U/ml of IFN- β (Fig. 2B and D).

3.3. Derivation of an equation that describes inhibition of HSV-1 by human IFN- β

The results of the previous experiment indicated that the logarithm of HSV-1 DNA yield, V , decreased as the logarithm of IFN concentration, I , was increased (Fig. 2C and D). Further analysis revealed that the relationship between V and I was described by

$$V(I) = V_{50} - \frac{\Delta V}{2} \tanh(x), \tag{1}$$

where $\tanh(x)$ is the hyperbolic tangent function $(e^x - e^{-x}) / (e^x + e^{-x})$ and x refers to the term $(I - I_{50}) / \Delta I$. The terms of Eq. (1) were initially derived from sigmoidal, IFN dose–response data sets by estimating the values of the four following parameters (Fig. 3A):

V_{\max} = log (maximum viral DNA yield) obtained when [IFN] is absent or negligible.

V_{\min} = log (minimum viral DNA yield) obtained when [IFN] is saturating.

I_{\min} \approx lowest log [IFN] at which log (viral DNA yield) deviates below V_{\max} .

I_{\max} \approx lowest log [IFN] at which log (viral DNA yield) approaches V_{\min} .

These parameters describe a rectangle with a width of $\Delta I \cdot 2$ and a height of ΔV whose center lies at the coordinates I_{50} , V_{50} , (Fig. 3A). The terms in the equation were estimated as follows:

$$\Delta V = V_{\max} - V_{\min}, \quad \Delta I = \frac{I_{\max} - I_{\min}}{2},$$

$$V_{50} = \frac{V_{\max} + V_{\min}}{2}, \quad I_{50} = \frac{I_{\max} + I_{\min}}{2}.$$

Eq. (1) states that

1. log (viral DNA yield) $\approx V_{\max}$ when log [IFN] $< I_{\min}$.
2. log (viral DNA) $\approx V_{\min}$ when log [IFN] $> I_{\max}$.
3. 76% of the decrease in log (viral DNA yield) occurs between I_{\min} and I_{\max} (Fig. 3A).

To illustrate the application of this equation, consider the HSV-1 DNA yields measured 30 h p.i. in Vero cells treated with 0.032 to 10,000 U/ml of IFN- β (Fig. 2C). Most of the decrease in viral DNA yields occurred between IFN- β concentrations of 10–1000 U/ml; thus, I_{\min} and I_{\max} were approximately 1.0 and 3.0, respectively (Fig. 2A). At negligible concentrations of IFN- β , viral DNA yields were ~ 600 times greater than the lower limit of detection of the assay, and thus V_{\max} was $\sim 2.78 = \log(600)$. At concentrations above 1000 U/ml,

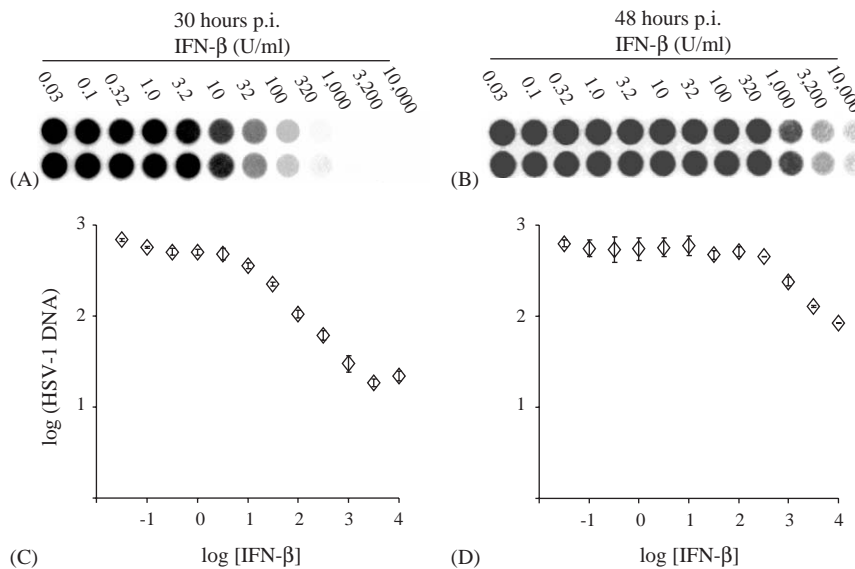


Fig. 2. Effect of human IFN- β on HSV-1 replication. (A) and (B) Dotblot of DNA samples harvested (A) 30 or (B) 48 h after inoculation with HSV-1 (MOI = 0.1). Vero cells were treated with half-log dilutions of human IFN- β ranging in concentration from 0.03 to 10,000 U/ml ($n = 2$ per concentration). HSV-1 DNA yields were measured based on the efficiency with which an HSV-specific oligonucleotide probe hybridized to each DNA sample. The log (viral DNA yield) measured (C) 30 or (D) 48 h after inoculation is plotted as a function of the log [IFN- β]. Open diamonds and error bars indicate the mean \pm SD of log (viral DNA yield), which is expressed in terms of log (fold-increase above the lower limit of detection); thus, the value '0' on the y-axis indicates the lower limit of detection.

HSV-1 DNA yields were ~20 times greater than the lower limit of detection, and thus V_{\min} was $\sim 1.30 = \log(20)$ (Fig. 2A). When these values were used, the

equation

$$V(\beta)^{30h} = 2.04 - 0.74 \tanh\left(\frac{\beta - 2.0}{1.0}\right)$$

was produced (dashed line in Fig. 3B). Using the method of least squares to refine estimates of ΔV , ΔI , V_{50} , and I_{50} by minimizing differences between the predicted and observed values, the equation

$$V(\beta)^{30h} = 1.99 - 0.78 \tanh\left(\frac{\beta - 2.08}{1.19}\right)$$

was obtained (solid line in Fig. 3B). Relative to the observed data, the $V(\beta)^{30h}$ equation accurately predicted how HSV-1 DNA yield changed as a function of IFN- β concentration (residual = 0.00 ± 0.01 ; $p > 0.2$ that Predicted–Observed = 0, two-tailed paired t -test). Likewise, an equation that described the effect of IFN- β on HSV-1 replication over a 48-h period was derived by applying these methods to the data in Fig. 2C. The initial estimates of I_{\min} , I_{\max} , V_{\min} , and V_{\max} (2.5, 4.0, 2.75, and 1.92) produced the equation

$$V(\beta)^{48h} \sim 2.34 - 0.41 \tanh\left(\frac{\beta - 3.25}{0.75}\right)$$

(dashed line in Fig. 3C). Once the method of least squares was used to fit the equation to the observed viral DNA yields, the equation

$$V(\beta)^{48h} = 2.30 - 0.45 \tanh\left(\frac{\beta - 3.16}{0.72}\right)$$

was obtained (solid line in Fig. 3C). Relative to the observed data, the $V(\beta)^{48h}$ equation accurately predicted how HSV-1 DNA yield changed as a function of IFN- β concentration (residual = 0.00 ± 0.01 ; $p > 0.2$ that $P - O = 0$, two-tailed paired t -test).

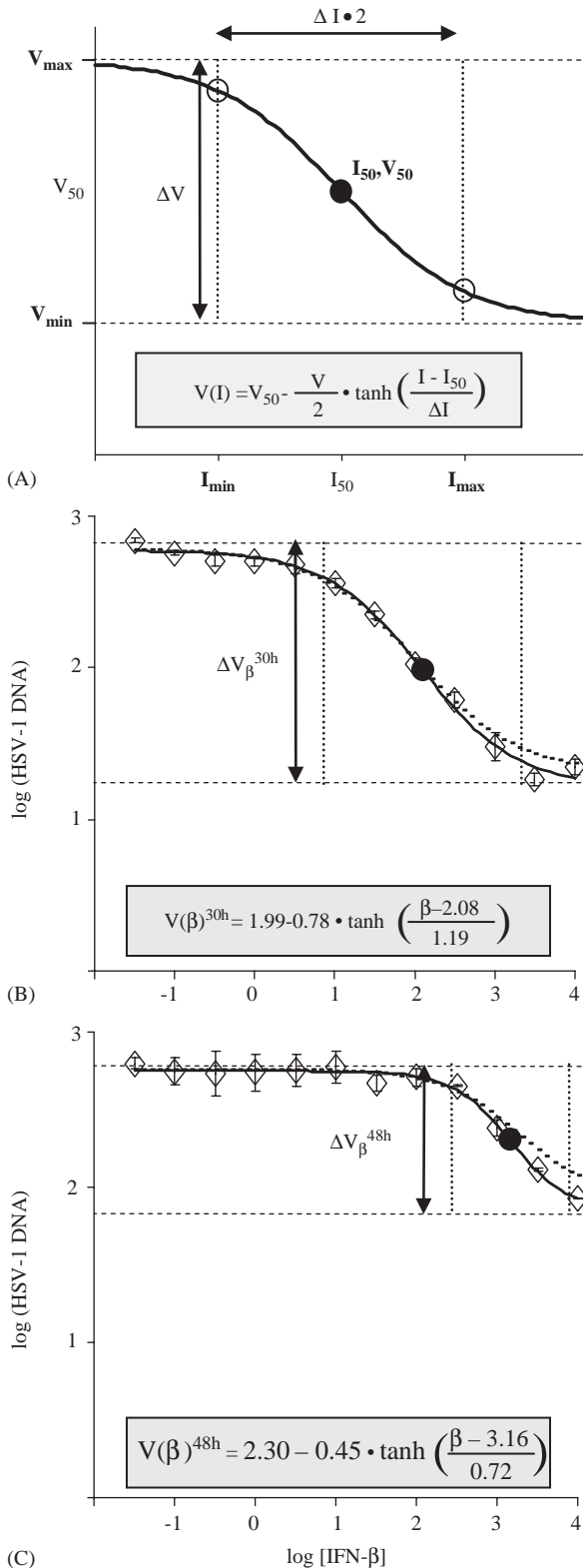


Fig. 3. Mathematical description of inhibition of HSV-1 replication by IFN- β . (A) The relationship between V (log [viral DNA yield]) and I (log [IFN]) is dictated by 1. ΔI , one-half the width of the difference between I_{\min} and I_{\max} , 2. ΔV , the height of the difference between V_{\max} and V_{\min} , and 3. the midpoint of the dose–response curve, I_{50} , V_{50} (closed circle). The locations of I_{\min} and I_{\max} are denoted by vertical dotted lines and the open circles on the dose–response curve. The upper and lower asymptotes of the hyperbolic tangent function, V_{\max} and V_{\min} respectively, are denoted by horizontal dashed lines. (B) and (C) Relationship of log (viral DNA yield) to log [IFN- β] when measured (B) 30 or (C) 48 h after inoculation. Open diamonds and error bars indicate the mean \pm SD of measured values of log (viral DNA yield), which are expressed as log (HSV-1 DNA). The dashed line indicates the simulated values that were derived by fitting the $V(\beta)$ equation to visual estimates of V_{\min} , V_{\max} , I_{\min} , and I_{\max} . The solid line indicates the simulated values derived by fitting the equation for (B) $V(\beta)^{30h}$ and (C) $V(\beta)^{48h}$ to their respective data sets by the method of least squares. The maximum reductions in log (viral DNA yield) achieved by IFN- β are denoted by the vertical arrows labeled ΔV_{β}^{30h} and ΔV_{β}^{48h} .

3.4. Derivation of an equation that describes inhibition of HSV-1 by human IFN- γ

Viral replication was compared in Vero cells inoculated with 0.1 PFU per cell of HSV-1 and which were treated with 0.032 to 10,000 U/ml of human IFN- γ . When infected cells were harvested 30 h p.i., IFN- γ concentrations as low as 1 U/ml had an effect on HSV-1 replication (Fig. 4A and C). Between doses of 1 and 100 U/ml, viral DNA yields decreased in proportion to the IFN- γ concentration in cell culture medium. IFN- γ concentrations of 100 U/ml or greater reduced HSV-1 DNA yields by ~5-fold (Fig. 4A and C). The effect of IFN- γ on HSV-1 replication over a 30-h period of infection was described by the equation,

$$V(\gamma)^{30h} = 2.30 - 0.36 \tanh\left(\frac{\gamma - 0.84}{1.21}\right).$$

When HSV-1 infected cells were harvested 48 h p.i., IFN- γ concentrations below 10 U/ml had no effect on viral DNA yields (Fig. 4B and D). As the IFN- γ concentration was increased from 10 to 100 U/ml, viral DNA yields decreased by ~3-fold (Fig. 4C and D). The effect of IFN- γ on HSV-1 replication over a 48-h period of infection was described by the equation,

$$V(\gamma)^{48h} = 2.56 - 0.22 \tanh\left(\frac{\gamma - 1.78}{0.74}\right).$$

Relative to the observed data, the $V(\gamma)^{30h}$ and $V(\gamma)^{48h}$ equations accurately predicted how HSV-1 DNA yield changed as a function of IFN- γ concentration (residual = 0.00 ± 0.01 ; in each case $p > 0.2$ that $P - O = 0$, two-tailed paired t -test). Thus, the first goal of the study was achieved and the individual effects of IFN- β and IFN- γ on HSV-1 replication were defined by the equations $V(\beta)$ and $V(\gamma)$, respectively.

3.5. Combined effects of IFN- β and IFN- γ on HSV-1: additive composite curve analysis

The second goal of the study was to test the null hypothesis that combinations of IFN- β and IFN- γ inhibit HSV-1 replication in a dose-additive manner. Additive composite curve analysis was used to test a specific prediction that follows from the null hypothesis: if the interaction is dose-additive, then a 1:1 combination of IFN- β and IFN- γ will reduce log (viral DNA yield) by the average of $V(\beta)$ and $V(\gamma)$ at all points along a dose-response curve (Tallarida, 2000, 2001; Tallarida et al., 1997). Therefore, viral replication was compared in Vero cells inoculated with 0.1 PFU per cell of HSV-1 and which were treated with 0.032 to 10,000 U/ml of IFN- β , IFN- γ , or 1:1 combinations of IFN- β and IFN- γ . When infected cells were harvested 30 h p.i., 10,000 U/ml of IFN- β or IFN- γ reduced HSV-1 DNA yields by a maximum of 42- and 6-fold, respectively (Fig. 5A and

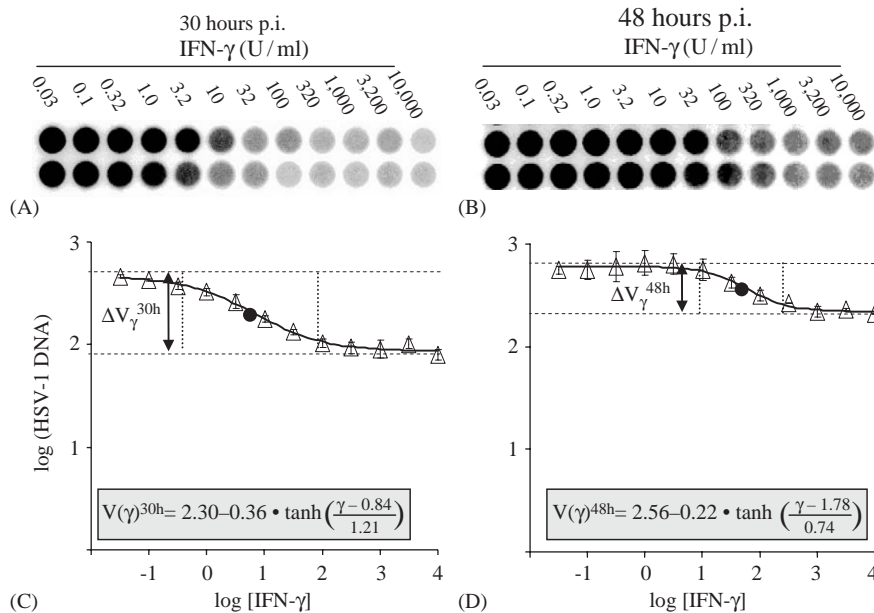


Fig. 4. Effect of human IFN- γ on HSV-1 replication. (A) and (B) Dotblot of DNA samples harvested (A) 30 or (B) 48 h after inoculation (MOI = 0.1). Vero cells were treated with half-log dilutions of IFN- γ ranging in concentration from 0.03 to 10,000 U/ml ($n = 2$ per concentration). (C) and (D) Relationship of log (viral DNA yield) to log [IFN- γ] when measured (C) 30 or (D) 48 h after inoculation. Open triangles and error bars indicate the mean \pm SD of measurements of log (viral DNA yield), which are expressed in terms of log (fold-increase above the lower limit of detection); thus, the value '0' on the y-axis indicates the lower limit of detection. The locations of I_{min} and I_{max} are denoted by vertical dotted lines, and V_{max} and V_{min} are denoted by horizontal dashed lines. The closed circle in the middle of the square indicates the location of I_{50} , V_{50} . The solid line indicates the simulated values derived by fitting the equation for (C) $V(\gamma)^{30h}$ or (D) $V(\gamma)^{48h}$ to their respective data sets by the method of least squares. The maximum reductions in log (viral DNA yield) achieved by IFN- γ are denoted by the vertical arrows labeled ΔV_{γ}^{30h} and ΔV_{γ}^{48h} .

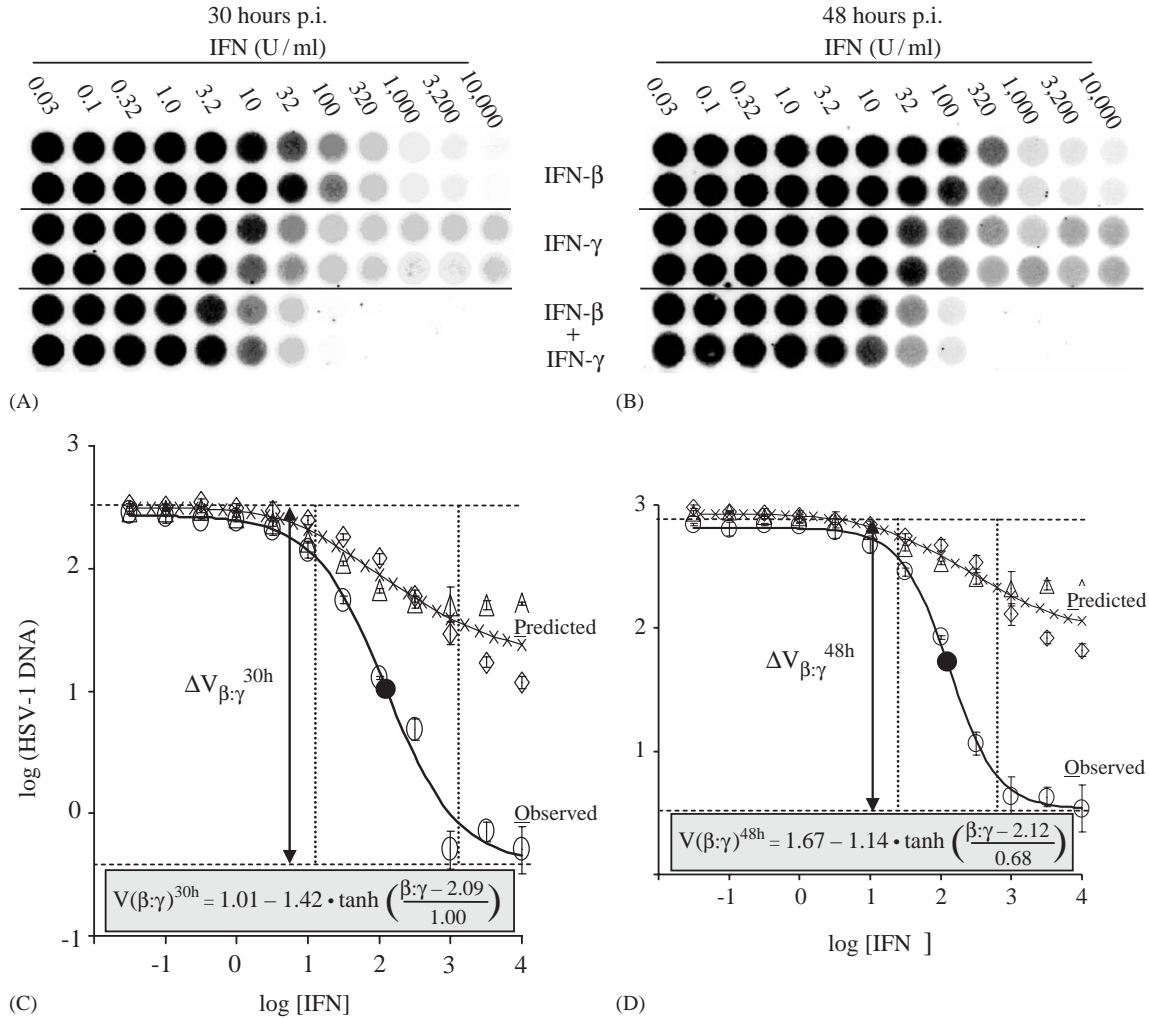


Fig. 5. Additive composite curve analysis of the combined effects of IFN- β and IFN- γ . (A) and (B) Dotplot of DNA samples harvested (A) 30 or (B) 48 h after inoculation (MOI = 0.1). Vero cells were treated with half-log dilutions of human IFN- β , human IFN- γ , or 1:1 combinations of IFN- β and IFN- γ that ranged in concentration from 0.03 to 10,000 U/ml ($n = 2$ per concentration). (C) and (D) Relationship of log (viral DNA yield) to log [IFN- β] (open diamonds), log [IFN- γ] (open triangles), or log [IFN- β + IFN- γ] (open circles) when measured (C) 30 or (D) 48 h after inoculation. Open symbols and error bars indicate the mean \pm SD of measurements of log (viral DNA yield), which are expressed in terms of log (fold-increase above the lower limit of detection); thus, the value '0' on the y-axis indicates the lower limit of detection. For the $V(\beta:\gamma)$ functions, the locations of I_{\min} and I_{\max} are denoted by vertical dotted lines, V_{\max} and V_{\min} are denoted by horizontal dashed lines, and the closed circle denotes the location of I_{50} . V_{50} . The line of X's indicates the reduction in log (viral DNA yield) predicted by the null (dose-additive) hypothesis. The solid black line indicates simulated values derived by fitting the equations (C) $V(\beta:\gamma)^{30h}$ or (D) $V(\beta:\gamma)^{48h}$ to the observed data. The maximum observed reductions in HSV-1 DNA yield achieved by 1:1 combinations of IFN- β + IFN- γ are denoted by the vertical arrows labeled $\Delta V_{\beta:\gamma}^{30h}$ and $\Delta V_{\beta:\gamma}^{48h}$.

C). The null hypothesis predicted that 1:1 combinations of IFN- β and IFN- γ should reduce HSV-1 DNA yields by a maximum of ~ 16 -fold (Fig. 5C). However, combinations of ≥ 500 U/ml each of IFN- β and IFN- γ reduced HSV-1 DNA yields to the lower limit of detection, and the dose-response curve was described by

$$V(\beta : \gamma)^{30h} = 1.01 - 1.42 \tanh\left(\frac{\beta : \gamma - 2.09}{1.00}\right)$$

(Fig. 5C). When cells were harvested 48 h p.i., 10,000 U/ml of IFN- β or IFN- γ reduced HSV-1 DNA yields by a maximum of 20- and 4-fold, respectively (Fig. 5B and D). The highest combined dose of IFN- β and IFN- γ

reduced HSV-1 DNA yields by 190-fold, and the dose-response curve was described by

$$V(\beta : \gamma)^{48h} = 1.67 - 1.14 \tanh\left(\frac{\beta : \gamma - 2.12}{0.68}\right).$$

Combinations of IFN- β and IFN- γ reduced HSV-1 DNA yields far beyond the predictions of the null hypothesis (30 h residual = -0.67 ± 0.15 , 48 h residual = -0.63 ± 0.14 ; $p < 0.0001$ that $P - O = 0$, two-tailed paired t -test). Thus, the combined effects of IFN- β and IFN- γ inhibited HSV-1 in a manner that was far greater than dose-additive.

Table 1
Individual versus combined effects of IFN-β and IFN-γ on HSV-1 replication

Hours p.i.	IFN ^a	Terms of $V(I)$ equation ^b				IC_{50} ^c	Maximum inhibition ^d
		ΔV	ΔI	V_{50}	I_{50}		
30	β ($n = 3$)	1.8 ± 0.3	1.2 ± 0.1	1.8 ± 0.2	2.4 ± 0.3	140–550	30–110
	γ ($n = 3$)	1.0 ± 0.4	0.9 ± 0.3	2.1 ± 0.3	1.2 ± 0.3	8–30	4–27
	1:1 $\beta + \gamma$ ($n = 2$)	2.7 ± 0.2	0.8 ± 0.2	1.2 ± 0.2	1.9 ± 0.3	30–160	320–780
48	β ($n = 3$)	1.0 ± 0.3	1.0 ± 0.3	2.3 ± 0.1	2.9 ± 0.2	550–1400	6–20
	γ ($n = 2$)	0.5 ± 0.1	0.9 ± 0.2	2.6 ± 0.1	1.7 ± 0.1	40–70	3–5
	1:1 $\beta + \gamma$ ($n = 2$)	2.4 ± 0.1	0.8 ± 0.1	1.6 ± 0.1	2.2 ± 0.1	130–170	180–280

^aInterferon used in dose–response experiments; n = the number of independent experiments performed. In each experiment, the range of [IFN] tested was 0.03 to 10,000 U/ml and was based on two replicate measurements at each dilution of IFN.

^bThe mean \pm SD of each term, as estimated in individual experiments by fitting Eq. (1) to the IFN dose–response data. The term ΔV = maximum reduction in log (viral DNA yield) and $\Delta I = 1/2(I_{\max} - I_{\min})$.

^c IC_{50} refers to the concentration at which a 50% reduction in log (HSV-1 DNA) was observed, and equals $10^{I_{50}}$. The IC_{50} is reported as the range of values that lie between $10^{\text{mean}-SD}$ of I_{50} and $10^{\text{mean}+SD}$ of I_{50} .

^d‘Maximum inhibition’ refers to the maximum observed reduction in log (HSV-1 DNA), and equals $10^{\Delta V}$. The maximum inhibition is reported as the range of values that lie between $10^{\text{mean}-SD}$ of ΔV and $10^{\text{mean}+SD}$ of ΔV .

Replicate experiments were performed to measure the mean \pm SD of the terms of $V(\beta)^{30h}$, $V(\beta)^{48h}$, $V(\gamma)^{30h}$, $V(\gamma)^{48h}$, $V(\beta:\gamma)^{30h}$ and $V(\beta:\gamma)^{48h}$ (Table 1). The terms I_{50} and ΔV are the most biologically relevant because the antilogs of these values (e.g. $10^{I_{50}}$ and $10^{\Delta V}$) equal the 50% inhibitory concentration (IC_{50}) and maximum fold-reduction, respectively, achieved by each IFN preparation. Comparison of the results obtained 30 h p.i. revealed that the IC_{50} of IFN-γ was ~10-fold lower than the IC_{50} of IFN-β (Table 1). However, the maximum reduction in HSV-1 DNA yields achieved by IFN-β was ~5-fold greater than that achieved by IFN-γ. Finally, the maximum reduction in log (viral DNA yield) achieved by a 1:1 combination of IFN-β and IFN-γ was not equal to the predicted dose-additive effect $(\Delta V_{\beta} + \Delta V_{\gamma})/2$. Rather, $\Delta V_{\beta:\gamma}$ was equal to $\Delta V_{\beta} + \Delta V_{\gamma}$ at 30 h p.i. (Table 1). Because the addition of logarithms is equal to multiplication on a linear scale, the results of additive composite curve analysis suggested that perhaps IFN-β and IFN-γ interact in a multiplicative manner to inhibit HSV-1 replication.

3.6. Combined effects of IFN-β and IFN-γ on HSV-1 replication: response surface analysis

The independent approach of response surface analysis was used to test the null hypothesis of dose-additivity, and this was achieved by measuring the effect of 64 unique dose combinations of IFN-β and IFN-γ on HSV-1 replication. Viral replication was compared 30 h p.i. in Vero cells inoculated with 0.1 PFU per cell and which were treated with an 8 × 8 matrix of IFN-β and IFN-γ concentrations (Fig. 6A). In the absence of IFN-γ, 10–1000 U/ml of IFN-β reduced HSV-1 DNA yields to a similar extent as observed in previous experiments, and thus as predicted by $V(\beta)^{30h}$ (Fig. 6B). In the

presence of 21 or 100 U/ml IFN-γ, 10–1000 U/ml of IFN-β reduced HSV-1 DNA yields with a potency that rapidly deviated from $V(\beta)^{30h}$, and instead approached the dose–response curve predicted by $V(\beta:\gamma)^{30h}$ (Fig. 6B). When a measure of inhibition, fold-reduction in HSV-1 DNA, was plotted as a function of [IFN-β] and [IFN-γ], the resulting response surface showed that combinations of IFN-β and IFN-γ inhibited HSV-1 replication with a potency that far exceeded the individual effects of IFN-β or IFN-γ alone (Fig. 6C).

When HSV-1 DNA yields were measured 48 h p.i., 1000 U/ml of IFN-β or IFN-γ alone caused only 3.4- and 2.1-fold reductions in HSV-1 DNA yields, respectively (Fig. 6D). In the absence of IFN-γ, 10–1000 U/ml of IFN-β reduced HSV-1 DNA yields to a similar extent as predicted by $V(\beta)^{48h}$ (Fig. 6E). In the presence of 21 or 100 U/ml IFN-γ, 10–1000 U/ml of IFN-β reduced HSV-1 DNA yields with a potency that rapidly deviated from $V(\beta)^{48h}$ and instead approached the dose–response curve predicted by $V(\beta:\gamma)^{48h}$ (Fig. 6E). When ‘fold-reduction in HSV-1 DNA’ was plotted as a function of [IFN-β] and [IFN-γ], the resulting response surface showed that combinations of IFN-β and IFN-γ inhibited HSV-1 replication with a potency that far exceeded the individual effects of IFN-β or IFN-γ alone (Fig. 6F). Therefore, the results of response surface analysis corroborated the conclusion that IFN-β and IFN-γ interact in a synergistic (i.e. greater than dose-additive) manner to inhibit HSV-1 replication.

4. Discussion

The first goal of this study, to define the individual effects of IFN-β or IFN-γ on HSV-1 replication, was

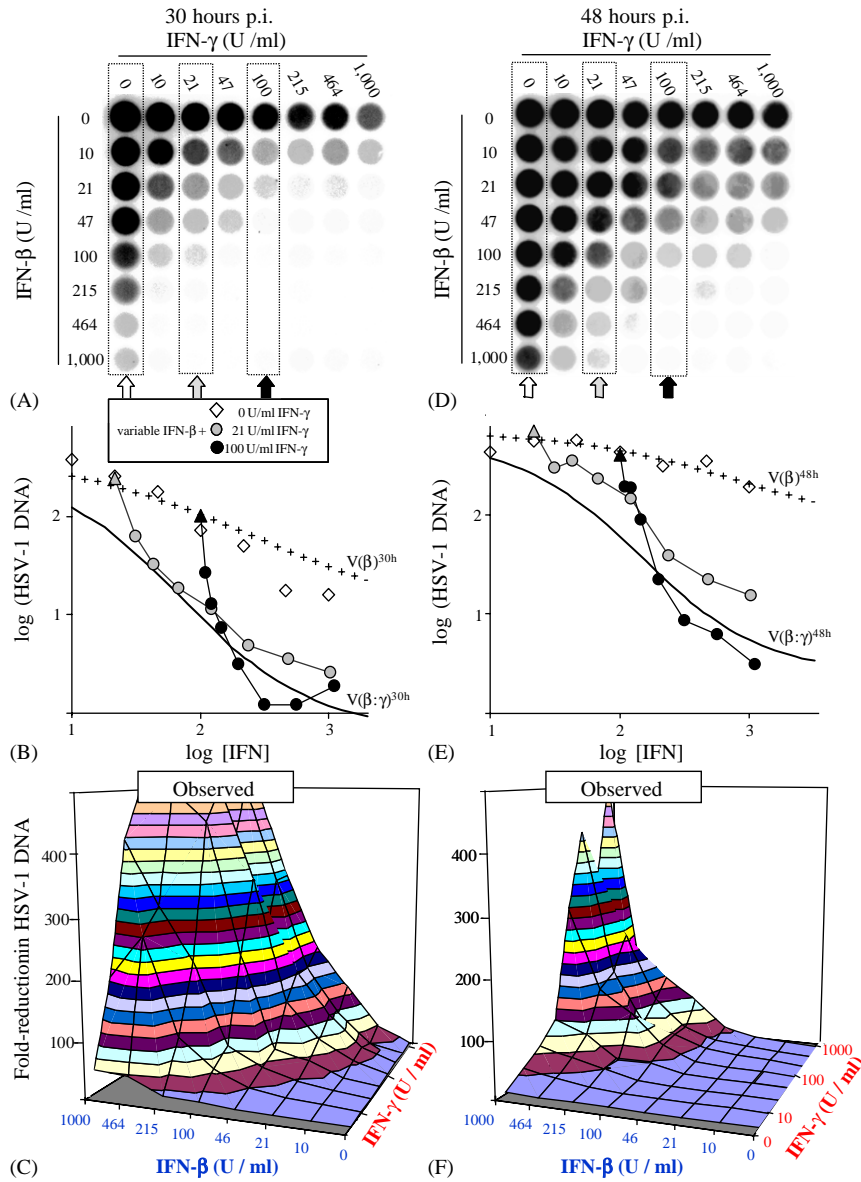


Fig. 6. Response surface analysis of the combined effects of IFN- β and IFN- γ . (A) and (D) Dotplot of DNA samples harvested (A) 30 h or (D) 48 h after inoculation (MOI = 0.1). Vero cells were treated with a matrix of 1/3rd log dilutions of IFN- β and IFN- γ that ranged in concentration from 0 to 1000 U/ml. (B) and (E) Relationship of log (HSV-1 DNA) to the combined concentration of IFN- β and IFN- γ in cultures treated with increasing doses of IFN- β and constant doses of IFN- γ of either 0, 21, or 100 U/ml, as determined (B) 30 h or (E) 48 h after inoculation. The equations $V(\beta)$ and $V(\beta:\gamma)$ provide reference points for previously observed effects of IFN- β versus 1:1 combinations of IFN- β and IFN- γ , and are based on the terms presented in Table 1. (C) and (F) The three-dimensional response surface of fold-reduction in HSV-1 DNA yield, as determined (C) 30 h or (F) 48 h after inoculation. Fold-reduction is defined as HSV-1 DNA yield in ‘vehicle-treated cells’/‘IFN-treated cells.’ Isoboles (contours) on the response surface occur in 20-fold increments.

achieved using the hyperbolic tangent function, $\tanh(x)$. The second goal, to determine if IFN- β and IFN- γ inhibit HSV-1 replication in a synergistic manner, was achieved using the methods of additive composite curve analysis and response surface analysis. Once we discuss why $\tanh(x)$ is relevant to a receptor-dependent process, we proceed to address the third goal of this study and define how IFN- β and IFN- γ interact to inhibit HSV-1 replication.

4.1. Individual effects of IFN- β or IFN- γ

Eq. (1),

$$V(I) = V_{50} - \frac{\Delta V}{2} \tanh(x)$$

was used in this study to describe how log (viral DNA), changes as a function of log [IFN]. The value of x in

tanh (x) is defined as

$$\left(\frac{I - I_{50}}{\Delta I}\right)$$

and describes how far log [IFN], or I , is away from the 50% inhibitory concentration in terms of the width of ΔI . For example, when $x = -2$, log [IFN] is too low to have a significant effect on HSV-1 replication because it is $2 \cdot \Delta I$ below I_{50} . Reciprocally, when $x = 2$, log [IFN] produces nearly 100% of its maximum inhibitory effect because it is $2 \cdot \Delta I$ above I_{50} .

The relevance of tanh (x) to a receptor-dependent process becomes more evident when the function is expressed in its full form,

$$\frac{e^x}{e^x + e^{-x}} - \frac{e^{-x}}{e^x + e^{-x}}$$

The first term $e^x/(e^x + e^{-x})$ represents the fraction of IFN receptors on the cell surface that are occupied by ligand, $R_{occupied}$. The second term $e^{-x}/(e^x + e^{-x})$ represents the fraction of IFN receptors that are available to bind ligand, R_{empty} . When expressed in this way, $\tanh(x) = R_{occupied} - R_{empty}$, which ranges in value from -1 when IFN ligand is absent to $+1$ when IFN ligand saturates all of the available receptors.

Applying this reasoning to the equation

$$V(I) = V_{50} - \frac{\Delta V}{2} \tanh(x)$$

it is instructive to consider the values of $V(I)$ obtained when log [IFN] equals I_{min} , I_{50} , and I_{max} (Fig. 3A). When

$$\log[\text{IFN}] = I_{min}, \quad x = \left(\frac{I_{min} - I_{50}}{\Delta I}\right) = -1,$$

$$R_{occupied} = \frac{e^{-1}}{e^{-1} + e^1} = 0.12,$$

$$R_{empty} = \frac{e^1}{e^{-1} + e^1} = 0.88$$

and thus $\tanh(x) = 0.12 - 0.88 = -0.76$. Consequently, $V(I_{min}) = V_{50} + 0.38 \cdot \Delta V$. In the second case, when

$$\log[\text{IFN}] = I_{50}, \quad x = \left(\frac{I_{50} - I_{50}}{\Delta I}\right) = 0,$$

$$R_{occupied} = R_{empty} = \frac{e^0}{e^0 + e^0} = \frac{1}{2}$$

and thus $\tanh(x) = 0.5 - 0.5 = 0$. Consequently, $V(I_{50}) = V_{50}$. Finally, when

$$\log[\text{IFN}] = I_{max}, \quad x = \left(\frac{I_{max} - I_{50}}{\Delta I}\right) = +1,$$

$R_{occupied} = 0.88$, $R_{empty} = 0.12$, and thus $\tanh(x) = 0.88 - 0.12 = 0.76$. Consequently, $V(I_{max}) = V_{50} - 0.38 \cdot \Delta V$.

Based on these definitions, it follows that 76% of the logarithmic reduction in viral DNA yield occurs as log [IFN] is increased from I_{min} to I_{max} (Fig. 3A).

Mathematical models are often limited by their practical utility or the compatibility of the terms in the equation with the underlying physical process. These considerations highlight two virtues of the proposed model. First, all of the parameters in the equation are readily estimated from IFN dose–response data. Second, tanh (x) provides an appropriate basis for describing the magnitude of a receptor-dependent effect. Given that the mathematical predictions are superimposable on the data, we conclude that

$$V(I) = V_{50} - \frac{\Delta V}{2} \tanh(x)$$

provides a valid model for describing the individual effects of IFN- β or IFN- γ on HSV-1 replication.

4.2. Combined effects of IFN- β and IFN- γ

The equations $V(\beta : \gamma)^{30h}$ and $V(\beta : \gamma)^{48h}$ describe how viral DNA yield changed as a function of IFN concentration in 1:1 combinations of IFN- β and IFN- γ (Fig. 5), but provide no basis for understanding how IFN- β and IFN- γ interact. Thus, an equation was developed that combines the individual effects of IFN- β and IFN- γ , and does so in a manner that accurately describes how combinations of these cytokines inhibit HSV-1 replication.

4.2.1. Derivation of a general $V(\beta + \gamma)$ equation

To combine the effects of IFN- β and IFN- γ in a single equation, it was necessary to re-state the $V(\beta)$ and $V(\gamma)$ equations such that decreases in viral DNA yield were expressed relative to a common reference point, V_{max} , as follows:

$$\begin{aligned} V(\beta) &= V_{max} - \Delta V_{\beta} \circ \alpha / \beta R_{occupied} \\ &= V_{max} - \Delta V_{\beta} \circ \left(\frac{e^{\beta}}{e^{\beta} + e^{-\beta}}\right) \end{aligned} \tag{2}$$

and

$$\begin{aligned} V(\gamma) &= V_{max} - \Delta V_{\gamma} \circ \gamma R_{occupied} \\ &= V_{max} - \Delta V_{\gamma} \circ \left(\frac{e^{\gamma}}{e^{\gamma} + e^{-\gamma}}\right). \end{aligned} \tag{3}$$

The term $\alpha / \beta R_{occupied}$ in Eq. (2) represents the fraction of activated IFN- α / β receptors, which ranges in value from 0 to 1, and is equal to $e^{\beta} / (e^{\beta} + e^{-\beta})$ where β is defined as $(\log[\text{IFN-}\beta] - \beta_{50}) / \Delta \beta$. Likewise, the term $\gamma R_{occupied}$ in Eq. (3) represents the fraction of activated IFN- γ receptors and is equal to $e^{\gamma} / (e^{\gamma} + e^{-\gamma})$ where γ is defined as $(\log[\text{IFN-}\gamma] - \gamma_{50}) / \Delta \gamma$. When re-stated in this way, $V(\beta)$ and $V(\gamma)$ return identical values to the

equations shown in Figs. 3 and 4. However, the modified forms of $V(\beta)$ and $V(\gamma)$ can be combined to yield a generic interaction model:

$$\begin{aligned}
 V(\beta + \gamma) &= V(\beta) + V(\gamma) \\
 &= V_{\max} - k_{\beta} \Delta V_{\beta} \left(\frac{e^{\beta}}{e^{\beta} + e^{-\beta}} \right) - k_{\gamma} \Delta V_{\gamma} \left(\frac{e^{\gamma}}{e^{\gamma} + e^{-\gamma}} \right).
 \end{aligned}
 \tag{4}$$

When IFN- γ is absent, Eq. (4) reduces to $V(\beta)$ (Eq. (2)). Reciprocally, when IFN- β is absent, Eq. (4) reduces to $V(\gamma)$ (Eq. (3)). The values of k_{β} and k_{γ} are what describe the interaction between IFN- β and IFN- γ . Below we consider two sets of values of k_{β} and k_{γ} that follow from the predictions that IFN- β and IFN- γ interact in a **1.** dose-additive or **2.** multiplicative manner.

4.2.2. Dose-additive model of the interaction between IFN- β and IFN- γ

When we assume that combinations of IFN- β and IFN- γ produce a dose-additive effect, we are assuming that IFN- β and IFN- γ are purely redundant. Thus, we predict that $k_{\beta} + k_{\gamma} = 1$, where k_{β} and k_{γ} are the fractional contributions of IFN- β and IFN- γ to the total dose. For example, if 10 U/ml IFN- β is combined with 100 U/ml IFN- γ , then

$$k_{\beta} = \frac{10}{10 + 100} = 0.09$$

and

$$k_{\gamma} = \frac{100}{10 + 100} = 0.91.$$

Inserting these assumptions into Eq. (4), we obtain a dose-additive model:

$$\begin{aligned}
 V(\beta + \gamma) &= V_{\max} - \frac{[\beta]}{[\beta] + [\gamma]} \Delta V_{\beta} \left(\frac{e^{\beta}}{e^{\beta} + e^{-\beta}} \right) \\
 &\quad - \frac{[\gamma]}{[\beta] + [\gamma]} \Delta V_{\gamma} \left(\frac{e^{\gamma}}{e^{\gamma} + e^{-\gamma}} \right).
 \end{aligned}
 \tag{5}$$

The model predicts that IFN- β and IFN- γ will inhibit HSV-1 replication by the average of their individual effects (Fig. 7A and B). The predictions of this model underestimate the observed potency with which combinations of IFN- β and IFN- γ inhibit HSV-1 replication (Fig. 6C and F).

4.2.3. Multiplicative model of the interaction between IFN- β and IFN- γ

If we assume that IFN- β and IFN- γ interfere with HSV-1 replication via independent mechanisms, then we assume that the inhibitory effects of IFN- β and IFN- γ are not redundant, but rather reinforce each other. If we assume complete independence, then it follows that k_{β} and k_{γ} both equal 1, and these terms drop out of Eq. (4)

to yield a multiplicative interaction model:

$$\begin{aligned}
 V(\beta + \gamma) &= \\
 &V_{\max} - \Delta V_{\beta} \left(\frac{e^{\beta}}{e^{\beta} + e^{-\beta}} \right) - \Delta V_{\gamma} \left(\frac{e^{\gamma}}{e^{\gamma} + e^{-\gamma}} \right).
 \end{aligned}
 \tag{6}$$

The response surface generated by the multiplicative interaction model is the result of plotting the sigmoid curve of the $V(\beta)$ function on top of, and at a right angle to, the sigmoid curve of the $V(\gamma)$ function (Fig. 7C and D). The result is that the general shape of the IFN- β dose-response curve remains identical at all doses of IFN- γ , but the amplitude of the IFN- β inhibition curve increases as the IFN- γ concentration is increased (Fig. 7C and D). Compared to the observed results (Fig. 6C and F), the multiplicative model accurately predicted the potency with which combinations of IFN- β and IFN- γ inhibited HSV-1 replication.

4.2.4. Fitting the multiplicative model to the response surface data

To generate the simulated response surfaces shown in Figs. 7C and D, the method of least squares was used to fit the terms of Eq. (6) to the observed viral DNA yields produced by combinations of IFN- β and IFN- γ at 30 and 48 h p.i. (Fig. 6A and D, respectively). The results of fitting Eq. (6) to the 30 h viral DNA yields (Fig. 6A) produced the following estimates of the six terms in the equation: $\Delta V_{\beta} = 1.71$, $\beta_{50} = 1.56$, $\Delta\beta = 0.73$, $\Delta V_{\gamma} = 1.18$, $\gamma_{50} = 1.19$, and $\Delta\gamma = 0.79$. The resulting values of ΔV_{β} , ΔV_{γ} , γ_{50} , and $\Delta\gamma$ correspond closely to the estimates of these values obtained by fitting Eq. (1) to the individual IFN- β or IFN- γ dose-response data. The values of β_{50} and $\Delta\beta$ corresponded closely to the values obtained with 1:1 combinations of IFN- β and IFN- γ (Table 1). Likewise, the fitting of Eq. (6) to 48 h viral DNA yields (Fig. 6D) generated values that were equivalent to earlier estimates of the same terms (Table 1). Thus, the observed response surfaces shown in Figs. 6C and F can effectively be predicted by combining the individual effects of IFN- β or IFN- γ (Table 1) in the multiplicative interaction model (Eq. (6)).

4.2.5. Predicted versus observed interaction of IFN- β and IFN- γ

The dose-additive and multiplicative interaction models provided two different interpretations of how the individual effects of IFN- β and IFN- γ might interact to reduce log (HSV-1 DNA yield) in infected cells. These mathematical predictions were compared to the observed combined effects of IFN- β and IFN- γ on log (HSV-1 DNA yield), as determined in response surface analysis experiments (Fig. 6A and D). The predictions of the dose-additive model consistently underestimated the efficacy with which combinations of IFN- β and IFN- γ actually reduced viral DNA yields (Fig. 7E and F). Based on the differences

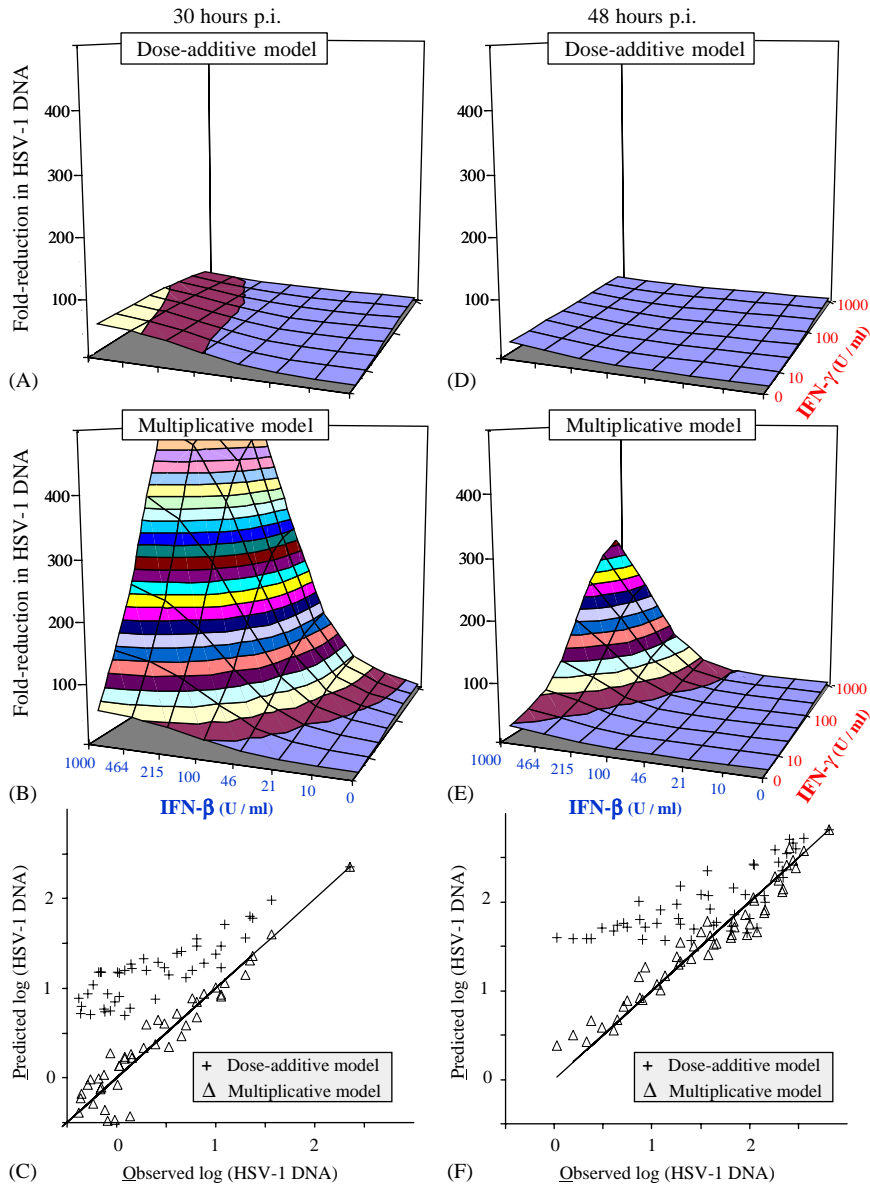


Fig. 7. Mathematical models of the interaction between IFN- β and IFN- γ . (A) and (B) Predictions of the dose-additive model (Eq. (5)). Three-dimensional response surfaces of fold-reduction in viral DNA yield predicted to occur (A) 30 h and (B) 48 h after inoculation if IFN- β and IFN- γ interact in a dose-additive manner. Isoholes on the response surface occur in 20-fold increments. (C) and (D) Predictions of the multiplicative interaction model (Eq. (6)). Three-dimensional response surfaces of fold-reduction in viral DNA yield that are predicted to occur (C) 30 h and (D) 48 h after inoculation if IFN- β and IFN- γ interact in a multiplicative manner. (E) and (F) Observed measurements of log (viral DNA yield) obtained (E) 30 h and (F) 48 h p.i. are plotted on the x-axis relative to the values predicted by the dose-additive and multiplicative interaction models (y-axis). The line of unity in each graph denotes the series of points at which there is a perfect correlation between predicted and observed values.

between the observed and predicted values (residuals = -0.47 ± 0.07 at 30 h p.i. and -0.91 ± 0.06 at 48 h p.i.), we reject the null hypothesis that IFN- β and IFN- γ interact in a dose-additive manner ($P < 0.0001$ that $P - O = 0$, two-tailed paired t -test). In contrast, the values of log (viral DNA yield) predicted by the multiplicative model correspond closely to the observed values (Fig. 7E and F). The residual differences between the predicted and observed data were -0.03 ± 0.03 at 30 h p.i. and 0.00 ± 0.00 at 48 h p.i. ($p > 0.2$, $P - O = 0$, two-tailed paired t -test). Therefore, we accept the hypothesis that

IFN- β and IFN- γ interact in a multiplicative manner to inhibit HSV-1 replication. This multiplicative interaction explains why combinations of IFN- β and IFN- γ can effectively stop HSV-1 replication, whereas IFN- β or IFN- γ alone do little more than delay the rate of viral spread.

4.3. Application of these methods to other systems

4.3.1. General

The function $y = \tanh(x)$ describes the sigmoidal data produced by measurements where the independent

variable, x , can be manipulated over an infinite range. The reason for the sigmoidal shape is that only a fixed range of changes in y (e.g. light absorbance or radioactivity) can be measured, and thus there are always lower and upper limits of detection (i.e. asymptotes). Most biologists cope with this physical reality by restricting their measurements to the “linear range” of the assay and describing their data with the linear equation $y = mx + b$. Of course, the linear range is simply the subset of $\tanh(x)$ that corresponds to the midpoint of the sigmoidal data set. If precision is required over the entire range of possible measurements, $\tanh(x)$ can be used. Our study is by no means the first time that $\tanh(x)$ has been applied to biological data (Anstey, 2003; Monteiro et al., 2002; Schisterman et al., 2003). However, most biologists are unaware that $\tanh(x)$ can be used to increase the reliability of routine quantitative assays (e.g. ELISA). If enough dilutions are included in a standard curve, the entire range of measurements between the lower and upper limits of detection can be defined with a generic form of Eq. (1)

$$y = y_{50} + \Delta y \tanh\left(\frac{x - x_{50}}{\Delta x}\right).$$

Of course, the purpose of a standard curve is not to describe the measured quantity y (e.g. optical density) in terms of x (e.g. cytokine abundance). Rather, the purpose is to extrapolate values of x in test samples from measurements of y . This is accomplished by inserting the measured values of y into the reciprocal equation,

$$x = x_{50} + \Delta x \operatorname{arctanh}\left(\frac{y - y_{50}}{\Delta y}\right),$$

where the constants Δx , Δy , x_{50} , and y_{50} are defined by the standard curve.

4.3.2. Pharmacological

Methods for defining the interaction between two biologically active agents are a topic of considerable debate (Berenbaum, 1989; Gebhart, 1992; Greco et al., 1995; Suhnel, 1990; Tallarida, 2000). The primary barrier we encountered in trying to address such a question was the development of an equation that accurately described the finite increase in inhibition (effect) that is produced over an infinite range of IFN concentration. The $\tanh(x)$ function provided a practical and precise solution to the problem, and allowed us to ultimately prove that IFN- β and IFN- γ interact in a multiplicative manner. The $\tanh(x)$ function should be useful in defining the finite effect of many drugs and agents over a wide range of concentrations. Therefore, we suspect that the generic interaction model presented in Eq. (4), which effectively combines the $\tanh(x)$ function for Agent 1 with the $\tanh(x)$ function for Agent 2, should be of general use in defining how other

biologically active substances interact to affect clinical relevant processes (e.g. pain management, antimicrobial therapy).

4.4. Implications of a multiplicative interaction between IFN- β and IFN- γ

A decade ago, Chisari and colleagues established the precedent that IFN- γ secreted by CD8⁺ T cells could synergize with a cytokine of the innate immune system, tumor necrosis factor (TNF)- α , to non-cytolytically suppress hepatitis B virus replication in liver cells in vivo (Guidotti et al., 1994, 1996, 1999). Likewise, there is considerable evidence that links CD8⁺ T cells and IFN- γ secretion to suppression of HSV-1 replication in the nervous system (Cantin et al., 1999a,b; Khanna et al., 2003; Liu et al., 2001, 2000, 1996; Simmons and Tschärke, 1992). In this context, IFN- γ may prevent the spread of HSV-1 infection in vivo by virtue of multiplying the potency with which IFN- α/β inhibit viral replication. Consistent with this hypothesis, combinations of IFN- β and IFN- γ disrupt productive HSV-1 replication in vitro by preventing viral DNA synthesis and nucleocapsid formation in infected cells (Pierce et al., submitted).

The observed synergy between IFN- α/β and IFN- γ may be important in innate resistance to HSV-1 infection, if natural killer cells or professional antigen-presenting cells serve as early sources of IFN- γ (Lieberman and Hunter, 2002; Suzue et al., 2003). Consistent with this hypothesis, mice that lack both IFN- α/β receptors and IFN- γ receptors (IFN α/β R^{-/-}, IFN γ R^{-/-} mice) experience explosive spread of HSV-1 infections (Luker et al., 2003). This phenotype is in stark contrast to IFN- α/β R^{-/-} mice or IFN- γ R^{-/-} mice, which are far more capable of limiting HSV-1 spread and generally survive infection despite the absence of one of the two IFN receptors (Luker et al., 2003). These results suggest that **1.** IFN- α/β and IFN- γ ligands are both available in HSV-1 infected animals to co-activate their receptors early in the infection and that **2.** there is enough redundancy between the IFN- α/β and IFN- γ pathways to protect IFN- γ R^{-/-} mice and IFN- α/β R^{-/-} mice from the devastating disease that would occur if both receptors were absent (e.g. both pathways lead to phosphorylation of Stat1). Consistent with this hypothesis, Stat1^{-/-} mice whose cells lack a key transcriptional activator of IFN-stimulated genes, experience uncontrolled spread of HSV-1 infection and die 6 to 7 days after corneal inoculation (Halford et al., unpublished data).

4.5. Physical basis of the multiplicative interaction between IFN- β and IFN- γ ?

Given the potency with which combinations of TNF- α and IFN- γ repress hepatitis B virus (Guidotti et al.,

1994) and cytomegalovirus (Lucin et al., 1994), the results of the current study raise questions about whether leukocyte-derived IFN- γ also multiplies the antiviral effects of TNF- α . However, the results of Chen et al. (1993) suggest an alternative interpretation. Chen et al. (1993) found that TNF- α and IFN- γ synergistically inhibit HSV-1 replication in corneal fibroblasts, but that this effect could be blocked with neutralizing antibody to IFN- β . Therefore, TNF- α and IFN- γ 's capacity to synergistically inhibit HSV-1 appears to be an indirect consequence of TNF- α 's recognized capacity to induce IFN- β secretion from human cells (Wolchok and Vilcek, 1992). It remains to be determined if IFN- β induction is also relevant to the mechanism by which TNF- α and IFN- γ synergistically inhibit the replication of hepatitis B virus and cytomegalovirus.

The mechanisms by which IFN- α/β and IFN- γ synergize to inhibit HSV-1 replication are not resolved. Although the IFN- α/β and IFN- γ signaling pathways are generally described as redundant, the results of this study indicate that another layer of complexity must exist. The fact that IFN- γ synergizes with stimuli such as bacterial lipopolysaccharide (a TNF- α inducer) in affecting cellular gene expression, has been attributed to cooperation between the downstream transcription factors of each pathway; Stat1 and NF- $\kappa\beta$, respectively (Ohmori et al., 1997; Paludan, 2000). However, such effects are complicated by the fact that lipopolysaccharide and TNF- α are also potent inducers of IFN- β (Chen et al., 1993; Karaghiosoff et al., 2003; Wolchok and Vilcek, 1992). We suspect that the results of the current study can be explained in a terms of a simpler explanation, which is that the IFN- α/β and IFN- γ signaling pathways cooperate in the formation of IFN-activated transcriptional complexes such as ISGF-3 and IRF-1 (Aaronson and Horvath, 2002; Levy and Darnell, 2002; Ramana et al., 2002). This hypothesis is consistent with the observation that the IFN- α/β receptors and IFN- γ receptors appear to be physically associated at the cell surface (Takaoka et al., 2000). Further work is necessary if we wish to understand the molecular basis by which the IFN- α/β and IFN- γ signaling pathways reinforce one another and the full biological significance of this observation.

Acknowledgements

The authors extend their appreciation to Ms. Jenifer Zinner for outstanding technical assistance and pedagogical guidance. This work was supported by a grant from the W.M. Keck Foundation of Los Angeles and the National Institutes of Allergy and Infectious Disease (AI 51414). Dr. William Halford is supported by a National Science Foundation EPSCoR grant to Montana State University (EPS 0346458).

References

- Aaronson, D.S., Horvath, C.M., 2002. A road map for those who don't know JAK-STAT. *Science* 296 (5573), 1653–1655.
- Anstey, C., 2003. A new model for the oxyhaemoglobin dissociation curve. *Anaesth. Intensive Care* 31 (4), 376–387.
- Balish, M.J., Abrams, M.E., Pumfery, A.M., Brandt, C.R., 1992. Enhanced inhibition of herpes simplex virus type 1 growth in human corneal fibroblasts by combinations of interferon-alpha and-gamma. *J. Infect. Dis.* 166 (6), 1401–1403.
- Berenbaum, M.C., 1989. What is synergy? *Pharmacol. Rev.* 41 (2), 93–141.
- Cantin, E., Tanamachi, B., Openshaw, H., 1999a. Role for gamma interferon in control of herpes simplex virus type 1 reactivation. *J. Virol.* 73 (4), 3418–3423.
- Cantin, E., Tanamachi, B., Openshaw, H., Mann, J., Clarke, K., 1999b. Gamma interferon (IFN-gamma) receptor null-mutant mice are more susceptible to herpes simplex virus type 1 infection than IFN-gamma ligand null-mutant mice. *J. Virol.* 73 (6), 5196–5200.
- Chee, A.V., Lopez, P., Pandolfi, P.P., Roizman, B., 2003. Promyelocytic leukemia protein mediates interferon-based anti-herpes simplex virus 1 effects. *J. Virol.* 77 (12), 7101–7105.
- Chehimi, J., Trinchieri, G., 1994. Interleukin-12: a bridge between innate resistance and adaptive immunity with a role in infection and acquired immunodeficiency. *J. Clin. Immunol.* 14 (3), 149–161.
- Chen, S.H., Oakes, J.E., Lausch, R.N., 1993. Synergistic anti-HSV effect of tumor necrosis factor alpha and interferon gamma in human corneal fibroblasts is associated with interferon beta induction. *Antiviral Res.* 22 (1), 15–29.
- Czarniecki, C.W., Fennie, C.W., Powers, D.B., Estell, D.A., 1984. Synergistic antiviral and antiproliferative activities of *Escherichia coli*-derived human alpha, beta, and gamma interferons. *J. Virol.* 49 (2), 490–496.
- Dressler, V., Muller, G., Suhnel, J., 1999. CombiTool—a new computer program for analyzing combination experiments with biologically active agents. *Comput. Biomed. Res.* 32 (2), 145–160.
- Farrar, M.A., Schreiber, R.D., 1993. The molecular cell biology of interferon-gamma and its receptor. *Annu. Rev. Immunol.* 11, 571–611.
- Gebhart, G.F., 1992. Comments on the isobole method for analysis of drug interactions. *Pain* 51 (3), 381; author reply 383–388.
- Greco, W.R., Bravo, G., Parsons, J.C., 1995. The search for synergy: a critical review from a response surface perspective. *Pharmacol. Rev.* 47 (2), 331–385.
- Guidotti, L.G., Ando, K., Hobbs, M.V., Ishikawa, T., Runkel, L., Schreiber, R.D., Chisari, F.V., 1994. Cytotoxic T lymphocytes inhibit hepatitis B virus gene expression by a noncytolytic mechanism in transgenic mice. *Proc. Natl Acad. Sci. USA* 91 (9), 3764–3768.
- Guidotti, L.G., Ishikawa, T., Hobbs, M.V., Matzke, B., Schreiber, R., Chisari, F.V., 1996. Intracellular inactivation of the hepatitis B virus by cytotoxic T lymphocytes. *Immunity* 4 (1), 25–36.
- Guidotti, L.G., Rochford, R., Chung, J., Shapiro, M., Purcell, R., Chisari, F.V., 1999. Viral clearance without destruction of infected cells during acute HBV infection. *Science* 284 (5415), 825–829.
- Halford, W.P., Gebhardt, B.M., Carr, D.J., 1996. Persistent cytokine expression in trigeminal ganglion latently infected with herpes simplex virus type 1. *J. Immunol.* 157 (8), 3542–3549.
- Karaghiosoff, M., Steinborn, R., Kovarik, P., Kriegshauser, G., Baccarini, M., Donabauer, B., Reichart, U., Kolbe, T., Bogdan, C., Leanderson, T., Levy, D., Decker, T., Muller, M., 2003. Central role for type I interferons and Tyk2 in lipopolysaccharide-induced endotoxin shock. *Nat. Immunol.* 4 (5), 471–477.
- Khanna, K., Bonneau, R., Kinchington, P., Hendricks, R., 2003. Herpes simplex virus-specific memory CD8(+) T cells are

- selectively activated and retained in latently infected sensory ganglia. *Immunity* 18 (5), 593–603.
- Koelle, D.M., Posavad, C.M., Barnum, G.R., Johnson, M.L., Frank, J.M., Corey, L., 1998. Clearance of HSV-2 from recurrent genital lesions correlates with infiltration of HSV-specific cytotoxic T lymphocytes. *J. Clin. Invest.* 101 (7), 1500–1508.
- Levy, D.E., Darnell Jr., J.E., 2002. Stats: transcriptional control and biological impact. *Nat. Rev. Mol. Cell Biol.* 3 (9), 651–662.
- Lieberman, L.A., Hunter, C.A., 2002. Regulatory pathways involved in the infection-induced production of IFN-gamma by NK cells. *Microbes Infect.* 4 (15), 1531–1538.
- Liu, T., Tang, Q., Hendricks, R.L., 1996. Inflammatory infiltration of the trigeminal ganglion after herpes simplex virus type 1 corneal infection. *J. Virol.* 70 (1), 264–271.
- Liu, T., Khanna, K.M., Chen, X., Fink, D.J., Hendricks, R.L., 2000. CD8(+) T cells can block herpes simplex virus type 1 (HSV-1) reactivation from latency in sensory neurons. *J. Exp. Med.* 191 (9), 1459–1466.
- Liu, T., Khanna, K.M., Carriere, B.N., Hendricks, R.L., 2001. Gamma interferon can prevent herpes simplex virus type 1 reactivation from latency in sensory neurons. *J. Virol.* 75 (22), 11178–11184.
- Lucin, P., Jonjic, S., Messerle, M., Polic, B., Hengel, H., Koszinowski, U.H., 1994. Late phase inhibition of murine cytomegalovirus replication by synergistic action of interferon-gamma and tumour necrosis factor. *J. Gen. Virol.* 75 (Part 1), 101–110.
- Luker, G.D., Prior, J.L., Song, J., Pica, C.M., Leib, D.A., 2003. Bioluminescence imaging reveals systemic dissemination of herpes simplex virus type 1 in the absence of interferon receptors. *J. Virol.* 77 (20), 11082–11093.
- MacLennan, I., Vinuesa, C., 2002. Dendritic cells, BAFF, and APRIL: innate players in adaptive antibody responses. *Immunity* 17 (3), 235–238.
- Matsumoto, M., Tanaka, N., Harada, H., Kimura, T., Yokochi, T., Kitagawa, M., Schindler, C., Taniguchi, T., 1999. Activation of the transcription factor ISGF3 by interferon-gamma. *Biol. Chem.* 380 (6), 699–703.
- Monteiro, L.H., Bussab, M.A., Chaui Berlink, J.G., 2002. Analytical results on a Wilson–Cowan neuronal network modified model. *J. Theor. Biol.* 219 (1), 83–91.
- Neumann-Haefelin, D., Sundmacher, R., Frey, H., Merk, W., 1985. Recombinant HuIFN-gamma prevents herpes simplex keratitis in African green monkeys: demonstration of synergism with recombinant HuIFN-alpha 2. *Med. Microbiol. Immunol. (Berl)* 174 (2), 81–86.
- Ohmori, Y., Schreiber, R.D., Hamilton, T.A., 1997. Synergy between interferon-gamma and tumor necrosis factor-alpha in transcriptional activation is mediated by cooperation between signal transducer and activator of transcription 1 and nuclear factor kappaB. *J. Biol. Chem.* 272 (23), 14899–14907.
- Paludan, S.R., 2000. Synergistic action of pro-inflammatory agents: cellular and molecular aspects. *J. Leukoc. Biol.* 67 (1), 18–25.
- Prichard, M.N., Shipman Jr., C., 1990. A three-dimensional model to analyze drug–drug interactions. *Antiviral Res.* 14 (4–5), 181–205.
- Prichard, M.N., Shipman Jr., C., 1990. *Antiviral Res.* 17 (1), 91–98.
- Ramana, C.V., Gil, M.P., Schreiber, R.D., Stark, G.R., 2002. Stat1-dependent and -independent pathways in IFN-gamma-dependent signaling. *Trends Immunol.* 23 (2), 96–101.
- Sainz Jr., B., Halford, W.P., 2002. Alpha/Beta interferon and gamma interferon synergize to inhibit the replication of herpes simplex virus type 1. *J. Virol.* 76 (22), 11541–11550.
- Schisterman, E.F., Moysich, K.B., England, L.J., Rao, M., 2003. Estimation of the correlation coefficient using the Bayesian approach and its applications for epidemiologic research. *BMC Med. Res. Methodol.* 3 (1), 5.
- Simmons, A., Tschärke, D.C., 1992. Anti-CD8 impairs clearance of herpes simplex virus from the nervous system: implications for the fate of virally infected neurons. *J. Exp. Med.* 175 (5), 1337–1344.
- Slinker, B.K., 1998. The statistics of synergism. *J. Mol. Cell Cardiol.* 30 (4), 723–731.
- Smith, K.O., 1964. Relationship between the envelope and the infectivity of herpes simplex virus. *Proc. Soc. Exp. Biol. Med.* 115, 814–816.
- Speck, P., Simmons, A., 1998. Precipitous clearance of herpes simplex virus antigens from the peripheral nervous systems of experimentally infected C57BL/10 mice. *J. Gen. Virol.* 79 (Part 3), 561–564.
- Suhnel, J., 1990. Evaluation of synergism or antagonism for the combined action of antiviral agents. *Antiviral Res.* 13 (1), 23–39.
- Suhnel, J., 1992. Comment on the paper: a three-dimensional model to analyze drug–drug interactions. *Antiviral Res.* 14, 181–206.
- Suzue, K., Asai, T., Takeuchi, T., Koyasu, S., 2003. In vivo role of IFN-gamma produced by antigen-presenting cells in early host defense against intracellular pathogens. *Eur. J. Immunol.* 33 (10), 2666–2675.
- Takaoka, A., Mitani, Y., Suemori, H., Sato, M., Yokochi, T., Noguchi, S., Tanaka, N., Taniguchi, T., 2000. Cross talk between interferon-gamma and -alpha/beta signaling components in caveolar membrane domains. *Science* 288 (5475), 2357–2360.
- Tallarida, R.J., 2000. *Drug Synergism and Dose-effect Analysis*. Chapman & Hall/CRC, New York.
- Tallarida, R.J., 2001. Drug synergism: its detection and applications. *J. Pharmacol. Exp. Ther.* 298 (3), 865–872.
- Tallarida, R.J., Stone Jr., D.J., Raffa, R.B., 1997. Efficient designs for studying synergistic drug combinations. *Life Sci.* 61 (26), L417–L425.
- Varinou, L., Ramsauer, K., Karaghiosoff, M., Kolbe, T., Pfeffer, K., Müller, M., Decker, T., 2003. Phosphorylation of the Stat1 transactivation domain is required for full-fledged IFN-gamma-dependent innate immunity. *Immunity* 19 (6), 793–802.
- Vilcek, J., Sen, J., 1996. Interferons and other cytokines. In: Fields, B.N., Knipe, D.M., Howley, P.M. (Eds.), *Virology*. Raven Publishers, Philadelphia, pp. 375–400.
- Vollstedt, S., Arnold, S., Schwerdel, C., Franchini, M., Alber, G., Di Santo, J.P., Ackermann, M., Suter, M., 2004. Interplay between alpha/beta and gamma interferons with B, T, and natural killer cells in the defense against herpes simplex virus type 1. *J. Virol.* 78 (8), 3846–3850.
- Wolchok, J.D., Vilcek, J., 1992. Induction of HLA class I mRNA by cytokines in human fibroblasts: comparison of TNF, IL-1 and IFN-beta. *Cytokine* 4 (6), 520–527.
- Zerial, A., Hovanessian, A.G., Stefanos, S., Huygen, K., Werner, G.H., Falcoff, E., 1982. Synergistic activities of type I (alpha, beta) and type II (gamma) murine interferons. *Antiviral Res.* 2 (4), 227–239.